Trans. Tianjin Univ. 2015, 21: 001-010
DOI 10.1007/s12209-015-2434-8

Novel Optimization Approach to Mixing Process Intensification*

Guo Kai(郭　凯)，Liu Botan(刘伯潭)，Li Qi(李　奇)，Liu Chunjiang(刘春江)
(State Key Laboratory of Chemical Engineering, School of Chemical Engineering and Technology, Tianjin University, Tianjin 300072, China)

Abstract: An approach was presented to intensify the mixing process. Firstly, a novel concept, the dissipation of mass transfer ability (DMA) associated with convective mass transfer, was defined via an analogy to the heat-work conversion. Accordingly, the focus on mass transfer enhancement can be shifted to seek the extremum of the DMA of the system. To this end, an optimization principle was proposed. A mathematical model was then developed to formulate the optimization into a variational problem. Subsequently, the intensification of the mixing process for a gas mixture in a micro-tube was provided to demonstrate the proposed principle. In the demonstration example, an optimized velocity field was obtained in which the mixing ability was improved, i.e., the mixing process should be intensified by adjusting the velocity field in related equipment. Therefore, a specific procedure was provided to produce a mixer with geometric irregularities associated with an ideal velocity.

Keywords: convective mass transfer; mass transfer ability; flow pattern optimization; calculus of variations; porous media model

In previous decades, the study of transport phenomena has become a fundamental engineering science field[1-3]. The influence of transport phenomena on equipment and process efficiency is so important that the investigation of a process intensification (PI) strategy has attracted considerable attention of many researchers in the chemical engineering community[4-7]. Among these related investigations, the optimization of transport phenomena has been a focus. Recently, the approach to analyzing and optimizing the chemical engineering process from the perspective of thermodynamics is noteworthy. Ever since Bejan[8-10] comprehensively illustrated that the second law of thermodynamics occupied a central place in the realm of heat transfer, the thermodynamic optimization principle of minimum entropy generation (MEG) has been developed and applied in the fields of industrial interest[11-18]. Besides, Guo *et al*[19] introduced the concept of entransy and entransy dissipation, and developed the entransy dissipation extremum (EDE) principle to optimize both the heat conduction and convective heat transfer. Since then, a series of studies were performed to optimize the convective heat transfer on EDE principle[20-23]. To perform the mass transfer enhancement, Chen *et al*[24,25] proposed the potential capacity dissipation function of mass transfer by extending the field synergy principle[26] to convective mass transfer. Liu *et al*[27] applied the thermodynamic optimization to constructing the optimal flow pattern for convective mass transfer, and then optimized the mixing equipment.

As demonstrated by previous experiments and analogy theories, the well-developed heat transfer theories can be extended to mass transfer analysis. Hence, the mass transfer performance can be related to the mass transfer ability, which will be irreversibly dissipated during mass transfer, corresponding to the destruction of available work in the heat-work conversion. Therefore, adjusting the dissipation of mass transfer ability (DMA) can be considered necessary to enhance the mass transfer. However, studies of the efficiency of convective mass transfer based on the irreversible dissipation of mass transfer ability have rarely been reported in literatures.

The objective of the present work was to propose an approach to convective mass transfer enhancement based on the concept of DMA. The exploration will proceed in

Accepted date: 2014-08-28.
*Supported by the National Basic Research Program of China ("973" Program, No. 2012CB720500) and the National Natural Science Foundation of China (No. 21176171).
Guo Kai, born in 1985, male, doctorate student.
Correspondence to Liu Chunjiang, E-mail: cjliu@tju.edu.cn.

the following steps. Firstly, the concept of DMA in convective mass transfer was proposed and its expression was derived. Then the optimization principle was necessarily developed to seek the extremum of the dissipation of mass transfer ability (EDMA). To this end, the corresponding computational fluid dynamics (CFD) model was developed by using the calculus of variations. Finally, the intensification of mixing process for a gas mixture was provided as a demonstration of the EDMA principle.

1 Analogy between heat-work conversion and convective mass transfer

According to the second law of thermodynamics, entropy generation is employed to measure the irreversibility of the process, and the lost available work is directly proportional to the entropy generation. For an inherently irreversible process, the lost available work is responsible for the reduced capacity of the heat energy converted to work. Similarly, the concept of the ability of mass transfer needs to be identified in the practical process. It is known that compared with laminar flow, the mass transfer occurring in turbulent flow manifests an enhanced mass transfer velocity due to the existence of turbulent eddies. The idealized eddy structure postulated in large eddy model and small eddy model can be viewed as a concomitant result of the turbulence structure. The interfacial convection in gas-liquid system can be illustrated as an alternative example. The instability due to mass transfer cited as Rayleigh or Marangoni effect will cause convection in the vicinity of the interface, and make the mass transfer velocity higher than that predicted by the classic theories. This indicates that the mass transfer performance in such a process is determined by convection rather than diffusion, which suggests that the mass transfer performance is related to the transfer mechanism. In other words, the mass transfer ability in convection is stronger than that in pure diffusion. The low mass transfer performance in the process governed by pure diffusion can be therefore attributed to the dissipation of mass transfer ability.

The potential mass transfer ability in a convective mass transfer process will be irreversibly dissipated due to the diffusion mechanism, which is similar in concept to the lost available work in a thermodynamic system. Analogous to the heat-work conversion, thus, the expression of DMA is derived. The analogies between the physical quantities for heat-work conversion and convective mass transfer are listed in Tab. 1.

Tab. 1 Physical quantities describing heat-work conversion and convective mass transfer

Heat-work conversion	Convective mass transfer
q	$q_{\mathrm{equ}}=-D\nabla(\rho c)$
k	$k_{\mathrm{equ}}=D$
T	$T_{\mathrm{equ}}=\rho c$
S	S_{equ}
$\dot{S}_{\mathrm{gen}}$	$\dot{S}_{\mathrm{gen,equ}}$

Note: ρ is the density; c is the mass fraction of species; and D is the molecular diffusive coefficient.

For the 2D infinitesimal control volume dxdy, the DMA per unit volume and per unit time can be expressed as follows:

$$\frac{\partial S_{\mathrm{gen,equ}}}{\partial t}\mathrm{d}x\mathrm{d}y=\frac{q_{\mathrm{equ},x}+\dfrac{\partial q_{\mathrm{equ},x}}{\partial x}\mathrm{d}x}{T_{\mathrm{equ}}+\dfrac{\partial T_{\mathrm{equ}}}{\partial x}\mathrm{d}x}\mathrm{d}y+$$
$$\frac{q_{\mathrm{equ},y}+\dfrac{\partial q_{\mathrm{equ},y}}{\partial y}\mathrm{d}y}{T_{\mathrm{equ}}+\dfrac{\partial T_{\mathrm{equ}}}{\partial y}\mathrm{d}y}\mathrm{d}x-\frac{q_{\mathrm{equ},x}}{T_{\mathrm{equ}}}\mathrm{d}y-\frac{q_{\mathrm{equ},y}}{T_{\mathrm{equ}}}\mathrm{d}x+$$
$$(s_{\mathrm{equ}}+\frac{\partial s_{\mathrm{equ}}}{\partial x}\mathrm{d}x)(u_x+\frac{\partial u_x}{\partial x}\mathrm{d}x)(\rho+\frac{\partial \rho}{\partial x}\mathrm{d}x)\mathrm{d}y+$$
$$(s_{\mathrm{equ}}+\frac{\partial s_{\mathrm{equ}}}{\partial y}\mathrm{d}y)(u_y+\frac{\partial u_y}{\partial y}\mathrm{d}y)(\rho+\frac{\partial \rho}{\partial y}\mathrm{d}y)\mathrm{d}x-$$
$$s_{\mathrm{equ}}u_x\rho\mathrm{d}y-s_{\mathrm{equ}}u_y\rho\mathrm{d}x+\frac{\partial(\rho s_{\mathrm{equ}})}{\partial t}\mathrm{d}x\mathrm{d}y \qquad (1)$$

where $S_{\mathrm{gen,equ}}$ is the DMA per unit volume; q_{equ} is the diffusive mass flux; T_{equ} is the concentration; s_{equ} is the potential mass transfer ability per unit mass; t is the time; and u_x and u_y are the velocity component in x and y directions, respectively. On the right side of Eq. (1), the first four terms represent the S_{equ} transfer associated with mass diffusion, the next four terms denote the S_{equ} convection into and out of the system, and the last term accounts for the time rate of S_{equ} accumulated in the control volume.

Divided by dxdy, Eq. (1) can be further reduced to

$$\frac{\partial S_{\mathrm{gen,equ}}}{\partial t}=\frac{1}{T_{\mathrm{equ}}}(\frac{\partial q_{\mathrm{equ},x}}{\partial x}+\frac{\partial q_{\mathrm{equ},y}}{\partial y})-$$
$$\frac{1}{T_{\mathrm{equ}}^2}(q_{\mathrm{equ},x}\frac{\partial T_{\mathrm{equ}}}{\partial x}+q_{\mathrm{equ},y}\frac{\partial T_{\mathrm{equ}}}{\partial y})+$$
$$s_{\mathrm{equ}}[\frac{\partial \rho}{\partial t}+u_x\frac{\partial \rho}{\partial x}+u_y\frac{\partial \rho}{\partial y}+\rho(\frac{\partial u_x}{\partial x}+\frac{\partial u_y}{\partial y})]+$$
$$\rho(\frac{\partial s_{\mathrm{equ}}}{\partial t}+u_x\frac{\partial s_{\mathrm{equ}}}{\partial x}+u_y\frac{\partial s_{\mathrm{equ}}}{\partial y}) \qquad (2)$$

The third term on the right-hand side of Eq. (2) vanishes based on the mass conservation equation:

$$\frac{\mathrm{D}\rho}{\mathrm{D}t}+\rho\nabla\cdot\boldsymbol{U}=0 \tag{3}$$

Eq. (2) then takes the following form:

$$\frac{\partial S_{\mathrm{gen,equ}}}{\partial t}=\frac{1}{T_{\mathrm{equ}}}\left(\frac{\partial q_{\mathrm{equ},x}}{\partial x}+\frac{\partial q_{\mathrm{equ},y}}{\partial y}\right)-$$

$$\frac{1}{T_{\mathrm{equ}}^2}\left(q_{\mathrm{equ},x}\frac{\partial T_{\mathrm{equ}}}{\partial x}+q_{\mathrm{equ},y}\frac{\partial T_{\mathrm{equ}}}{\partial y}\right)+\rho\frac{\mathrm{D}s_{\mathrm{equ}}}{\mathrm{D}t} \tag{4}$$

According to the definition of the substantial derivative, the following relationships can be obtained:

$$\delta Q_{\mathrm{equ}}=T_{\mathrm{equ}}\mathrm{d}S_{\mathrm{equ}}=T_{\mathrm{equ}}\mathrm{d}(\rho s_{\mathrm{equ}}) \tag{5}$$

$$\rho\frac{\mathrm{D}s_{\mathrm{equ}}}{\mathrm{D}t}=\frac{\mathrm{D}S_{\mathrm{equ}}}{\mathrm{D}t}-s_{\mathrm{equ}}\frac{\mathrm{D}\rho}{\mathrm{D}t}=\frac{\mathrm{D}Q_{\mathrm{equ}}}{T_{\mathrm{equ}}\mathrm{D}t}-s_{\mathrm{equ}}\frac{\mathrm{D}\rho}{\mathrm{D}t} \tag{6}$$

$$\frac{\mathrm{D}Q_{\mathrm{equ}}}{\mathrm{D}t}=-\left(\frac{\partial q_{\mathrm{equ},x}}{\partial x}+\frac{\partial q_{\mathrm{equ},y}}{\partial y}\right) \tag{7}$$

where S_{equ} represents the potential mass transfer ability per unit volume; and Q_{equ} denotes the mass per unit volume associated with the diffusion alone.

By employing Eqs. (6)—(7) in Eq. (4), $\dot{S}_{\mathrm{gen,equ}}$ can be conveniently rearranged as follows:

$$\frac{\partial S_{\mathrm{gen,equ}}}{\partial t}=-\frac{1}{T_{\mathrm{equ}}^2}\left(q_{\mathrm{equ},x}\frac{\partial T_{\mathrm{equ}}}{\partial x}+q_{\mathrm{equ},y}\frac{\partial T_{\mathrm{equ}}}{\partial y}\right)-s_{\mathrm{equ}}\frac{\mathrm{D}\rho}{\mathrm{D}t}=$$

$$\frac{k_{\mathrm{equ}}}{T_{\mathrm{equ}}^2}(\nabla T_{\mathrm{equ}}\cdot\nabla T_{\mathrm{equ}})-s_{\mathrm{equ}}\frac{\mathrm{D}\rho}{\mathrm{D}t}=$$

$$\frac{D}{(\rho c)^2}(\nabla\rho c\cdot\nabla\rho c)-s_{\mathrm{equ}}\frac{\mathrm{D}\rho}{\mathrm{D}t} \tag{8}$$

The present study assumed incompressible flow, which satisfies:

$$\frac{\mathrm{D}\rho}{\mathrm{D}t}=0 \tag{9}$$

Finally, the DMA can be expressed as

$$\frac{\partial S_{\mathrm{gen,equ}}}{\partial t}=\frac{D}{(\rho c)^2}(\nabla\rho c\cdot\nabla\rho c) \tag{10}$$

As discussed above, the magnitude of DMA is related to the mass transfer ability. Therefore, considerable motives exist to develop an approach to seeking the extremum of the DMA of a process, so that mass transfer process can be improved.

2 Mass transfer enhancement based on the EDMA principle

Since the experiment of mass transfer is usually known to be expensive and laborious, the use of numerical simulation is a good alternative. Generally, the mathematical modeling and simulation of the convective mass transfer is well accomplished by using CFD. On close inspection of the published literatures, the numerical results solved by CFD proved to be in good agreement with experimental data. In this study, CFD modeling for optimizing convective mass transfer was performed based on the EDMA principle.

For a given set of boundary conditions, the mixing performance is determined by the velocity field. In other words, the process will be improved when the mass transfer is performed under an ideal velocity field. Hence, in this study, the velocity field was treated as an independent argument function in the optimization.

2.1 Objective function

The object here is to find the velocity distribution to get the extremum of the DMA of a system. Therefore, the global DMA is employed as the objective function.

$$J=\iiint_{\Omega}\frac{D(\nabla\rho c\cdot\nabla\rho c)}{(\rho c)^2}\mathrm{d}V \tag{11}$$

2.2 Basic equations

For laminar steady incompressible flow, the governing equations of convective mass transfer are summarized as follows:

$$\nabla\cdot\boldsymbol{U}=0 \tag{12}$$

$$\nabla\cdot(\rho\boldsymbol{U}\boldsymbol{U})=-\nabla P+\nabla\cdot\mu(\nabla\boldsymbol{U}+\nabla\boldsymbol{U}^{\mathrm{T}})+F \tag{13}$$

$$\rho\boldsymbol{U}\cdot\nabla c-\nabla\cdot(D\nabla\rho c)=0 \tag{14}$$

2.3 Constraints

For practical considerations, the viscous dissipation needs to be suitably limited so that the system designed in accordance with an optimized velocity field can be easily extended to applications with specified operating conditions. Thus, the viscous dissipation is necessarily predetermined over an appropriate range which is relevant to the practical problem. The viscous dissipation function is defined as follows:

$$\phi=\mu(\nabla\boldsymbol{U}+\nabla\boldsymbol{U}^{\mathrm{T}}-\frac{2}{3}\boldsymbol{I}\nabla\cdot\boldsymbol{U}):\nabla\boldsymbol{U} \tag{15}$$

where $\boldsymbol{I}$ is the unit tensor; and μ is the molecular viscosity.

The constraint of the viscous dissipation can be expressed as

$$\iiint_{\Omega}\phi\mathrm{d}V=\text{Constant} \tag{16}$$

This viscous dissipation constraint can be regarded as a limitation specified for the external power consumption or pressure drop. Additionally, the conservation of mass and species is also considered as constraints in the

optimization.

2.4 Statement of the enhancement for convective mass transfer

When considering the objective function, argument function and constraints, the optimization can be conveniently addressed as a typical variational problem. Therefore, a Lagrange multiplier equation is constructed:

$$\Pi = \iiint_{\Omega} \{ \frac{D\nabla\rho c \cdot \nabla\rho c}{(\rho c)^2} + A\nabla \cdot \boldsymbol{U} + B[\rho \boldsymbol{U} \cdot \nabla c - \nabla \cdot (D\nabla\rho c)] + C\phi \} \mathrm{d}V \quad (17)$$

where A, B and C are Lagrange multipliers. Because of different types of constraints, A and B vary with positions, while C is constant for a given viscous dissipation rate.

For a binary-component system, the density of the gas mixture is defined by the ideal gas law for incompressible flow:

$$\rho = \frac{p}{RT\sum_{\alpha}\frac{c_{\alpha}}{M_{\mathrm{w},\alpha}}} = \frac{pM_{\mathrm{w},1}M_{\mathrm{w},2}}{RT(M_{\mathrm{w},1} - c_1 M_{\mathrm{w},1} + c_1 M_{\mathrm{w},2})} = \frac{C_{\rho}}{M_{\mathrm{w},1} - c_1 M_{\mathrm{w},1} + c_1 M_{\mathrm{w},2}} \quad (18)$$

where R is the universal gas constant; p is the pressure; M_{w} is the molecular weight; T is the temperature; and C_{ρ} is the constant.

The viscosity of the mixture is defined as follows:

$$\mu = \frac{c_1\mu_1 M_{\mathrm{w},1}^{0.5} M_{\mathrm{w},2} + (M_{\mathrm{w},1} - c_1 M_{\mathrm{w},1}) M_{\mathrm{w},2}^{0.5}\mu_2}{c_1 M_{\mathrm{w},1}^{0.5} M_{\mathrm{w},2} + (M_{\mathrm{w},1} - c_1 M_{\mathrm{w},1}) M_{\mathrm{w},2}^{0.5}} \quad (19)$$

where $M_{\mathrm{w},i}$, c and μ_i are molecular weight, mass fraction and molecular viscosity of species i, respectively.

The variation of Eq. (17) is the mass continuity equation with respect to A and the conservation equation of species with respect to B.

The variation of Eq. (17) with respect to the velocity vector $\boldsymbol{U}$ yields the following:

$$-\frac{B\rho\nabla c}{2C} + \frac{\rho\nabla A}{2C} + \nabla \cdot \mu(\nabla \boldsymbol{U} + \nabla \boldsymbol{U}^{\mathrm{T}}) + \nabla \cdot (\rho \boldsymbol{U}\boldsymbol{U}) = \nabla \cdot (\rho \boldsymbol{U}\boldsymbol{U}) \quad (20)$$

When comparing the momentum equation and substituting A with

$$\nabla A = -\frac{2C}{\rho}\nabla p \quad (21)$$

Eq. (20) can be rewritten as the momentum equation with a virtual volume force F:

$$F = -\frac{B\rho\nabla c}{2C} + \nabla \cdot (\rho \boldsymbol{U}\boldsymbol{U}) \quad (22)$$

Essentially, the momentum equation with a virtual volume force is the Euler-Lagrange equation, whose solution is selected out of all admissible argument functions to obtain the extremum of the objective function under given constraints.

The variation of Eq. (17) with respect to mass fraction yields the following:

$$\begin{aligned}\nabla \cdot \left(\rho D\nabla B\right) + \frac{(M_{\mathrm{w},1} - cM_{\mathrm{w},1} + cM_{\mathrm{w},2})}{M_{\mathrm{w},1}}\rho \boldsymbol{U}\nabla \cdot B = {} & D\nabla\rho \cdot \nabla B + \frac{2D(\nabla c \cdot \nabla c)}{c^3} \cdot \\ & \frac{(M_{\mathrm{w},1} - cM_{\mathrm{w},1} + cM_{\mathrm{w},2})}{M_{\mathrm{w},1}} - \\ & \frac{2(M_{\mathrm{w},1} - cM_{\mathrm{w},1} + cM_{\mathrm{w},2})}{M_{\mathrm{w},1}c^2}\boldsymbol{U} \cdot \nabla c + \\ & \frac{6D(M_{\mathrm{w},1} - M_{\mathrm{w},2})}{M_{\mathrm{w},1}c^2}\nabla c \cdot \nabla c + \\ & \frac{6D}{M_{\mathrm{w},1}c}\frac{(M_{\mathrm{w},1} - M_{\mathrm{w},2})^2}{(M_{\mathrm{w},1} - cM_{\mathrm{w},1} + cM_{\mathrm{w},2})}\nabla c \cdot \nabla c - \\ & \frac{2(M_{\mathrm{w},1} - M_{\mathrm{w},2})}{M_{\mathrm{w},1}c}\boldsymbol{U} \cdot \nabla c + \\ & \frac{2D(M_{\mathrm{w},1} - M_{\mathrm{w},2})^3}{M_{\mathrm{w},1}(M_{\mathrm{w},1} - cM_{\mathrm{w},1} + cM_{\mathrm{w},2})^2}\nabla c \cdot \nabla c + \\ & 2C\frac{(M_{\mathrm{w},1} - M_{\mathrm{w},2})}{M_{\mathrm{w},1}}\nabla p \cdot \boldsymbol{U} + \\ & C\left\{\frac{M_{\mathrm{w},1}^{0.5}M_{\mathrm{w},2}^{1.5}(M_{\mathrm{w},1} - cM_{\mathrm{w},1} + cM_{\mathrm{w},2})(\mu_1 - \mu_2)}{\left[cM_{\mathrm{w},1}^{0.5}M_{\mathrm{w},2} + \left(M_{\mathrm{w},1} - cM_{\mathrm{w},1}\right)M_{\mathrm{w},2}^{0.5}\right]^2}\right\} \cdot \\ & (\nabla \boldsymbol{U} + \nabla \boldsymbol{U}^{\mathrm{T}}) : \nabla \boldsymbol{U}\end{aligned} \quad (23)$$

The boundary conditions for multiplier B are summarized as follows:

(1) For a non-slip wall and pressure outlet

$$\frac{\partial B}{\partial x_n} = 0$$

where x_n is the coordinate normal to the surface.

(2) For a velocity inlet

$$B = 0$$

The numerical solution of Eqs. (12)—(14), (22)—(23) denotes the ideal velocity field subject to given viscous dissipation.

3 Numerical example and discussion

A specific mixing process for a CO_2-air gas mixture

was presented to demonstrate the EDMA principle and the CFD model. Here, the problem was confined to the laminar steady flow of an incompressible ideal gas mixture. Viscous heating was not considered. In addition, the mixing process was assumed to be isothermal, and the physical properties (density and viscosity) were assumed to depend on the composition only. The binary-component diffusion coefficient was constant for the sake of simplicity. The Kundsen number[28], Kn, can be used to classify fluids that deviate from continuum behavior[29]. For the concerned mixing process, the fluid can be treated as a continuum with a small Kn ($Kn \leqslant 10^{-3}$).

The sketch of the tube is shown in Fig. 1. The diameter of the tube is 1 mm and its length is 6 mm. It consists of three sections: entry section, middle section and exit section. The length for each section is 1.5 mm, 2.0 mm and 2.5 mm, respectively. To avoid boundary effects that influence the optimized flow pattern, only the middle section is optimized. The mass flow rate is 0.2×10^{-5} kg/s, corresponding to an average Re of 150.85. The density and viscosity of the gas mixture are determined by Eq. (18) and Eq. (19), respectively. The diffusion coefficient D of CO_2 in air is 1.381×10^{-5} m^2/s [30]. The CFD code Fluent 6.3.26 is utilized in our numerical computation. The velocity and pressure are linked by using the SIMPLE algorithm, and the convection and diffusion terms are discretized by using the QUICK scheme.

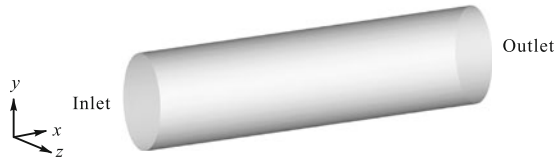

Fig. 1 Sketch of the micro round tube

3.1 Boundary conditions

The boundary conditions for simulation are listed as follows.

At velocity inlet,

$$u_{\text{in}} = u_0$$

where u_{in} is the velocity component normal to the inlet.

For the mass fraction of CO_2 at the inlet, the following condition is imposed:

$$\begin{cases} c = 0.95, & r < 0.000\,2 \\ c = 0.05, & r \geqslant 0.000\,2 \end{cases}$$

where r is the radial distance from the centerline.

At pressure outlet,

$$p = p_0$$

A non-slip boundary condition is prescribed for the walls:

$$u_{i|\text{wall}} = 0\,;\ \frac{\partial c_\alpha}{\partial x_n} = 0$$

The symmetry condition is defined as follows:

$$\frac{\partial u_i}{\partial x_n} = 0\,;\ \frac{\partial c_\alpha}{\partial x_n} = 0$$

3.2 Numerical simulation results

The dependence of the numerical simulation results on the grid resolution was verified, and the cell number of 810 810 was adopted in the physical model. As shown in Fig. 2 and Fig. 3, the concentration field and spatial streamlines in the optimized flow pattern are approximately symmetric. Accordingly, a quarter of the tube was employed as a physical model in the following calculations to provide an appropriate compromise between the simulation accuracy and computation expense. The mesh of the model is shown in Fig. 4. The number of cells in the grid was approximately 194 400.

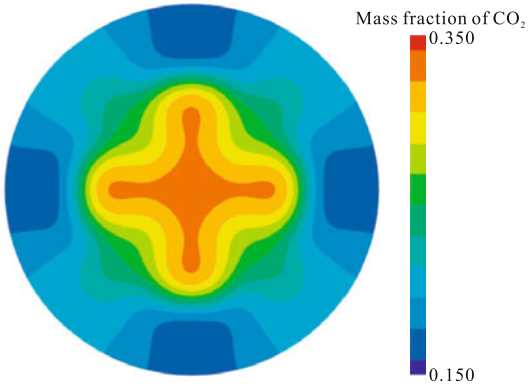

Fig. 2 Concentration field of CO_2 in the cross-section at x=2.5 mm in the optimized flow pattern in the physical model (a complete tube)

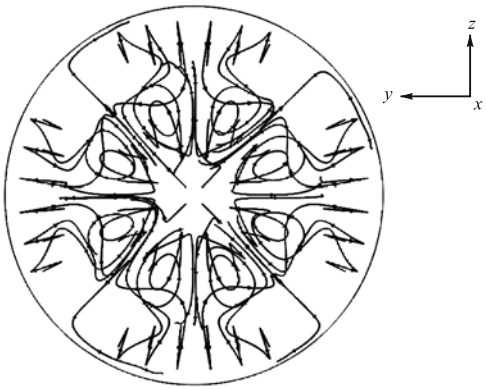

Fig. 3 Streamlines in the optimized flow pattern in the physical model (a complete tube)

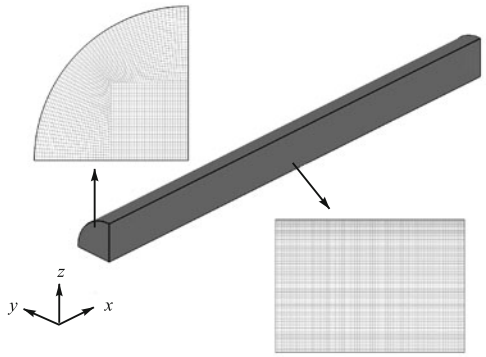

Fig. 4 Grid generation strategy

As a basis for comparison, the original flow pattern was simulated by solving Navier-Stokes equation while F=0. As seen from Fig. 5, the radial velocity was negligibly small compared with axial velocity, and a large concentration gradient existed in the radial direction. Then, the virtual volume force was introduced, and resulted in an optimized flow pattern. As shown in Fig. 6, the vortices were generated to force the formation of radial convection and thus prompted the mixing.

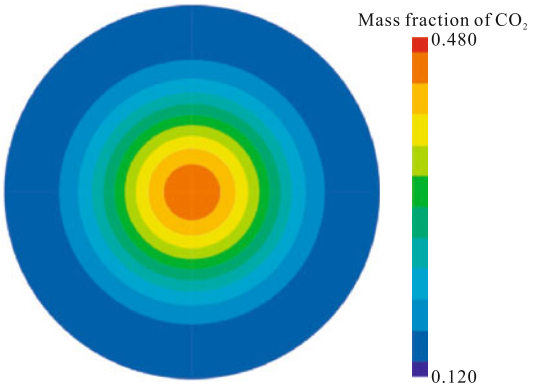

(a) Concentration field of CO_2

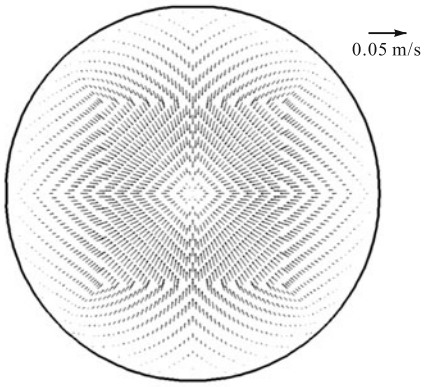

(b) Velocity field

Fig. 5 Concentration field of CO_2 and velocity field in the cross-section (x=2.5 mm) in the original flow pattern

The mixing length[31] was employed in accessing the mixing efficiency. The gas mixture was considered to be completely mixed when the mean value of the concentration field was achieved for all locations in a certain cross-section. Here, complete mixing was assumed to be achieved when all the local mass fractions deviated by no more than 5% from the mean value. The mixing length was the distance between the inlet and the transverse plane where complete mixing was achieved.

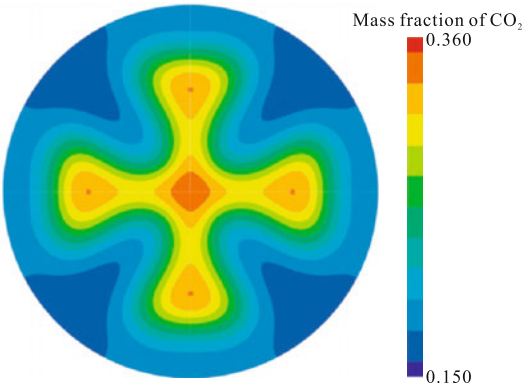

(a) Concentration field of CO_2

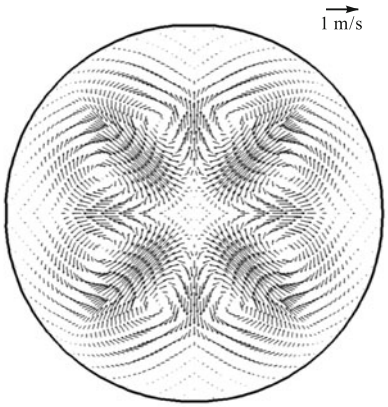

(b) Velocity field

Fig. 6 Concentration field of CO_2 and velocity field in the cross-section (x=2.5 mm) in the optimized flow pattern

The calculations show that the complete mixing was not achieved in the original velocity field, while it was achieved in the optimized flow pattern with a mixing length of 5.204 mm. Simultaneously, the total viscous dissipation rate increased from 3.282×10^{-6} W to 6.649×10^{-6} W. By changing the value of the multiplier C, the variation of mixing length with viscous dissipation rate is shown in Fig. 7, which shows that the total viscous dissipation rate negatively correlates with the mixing length.

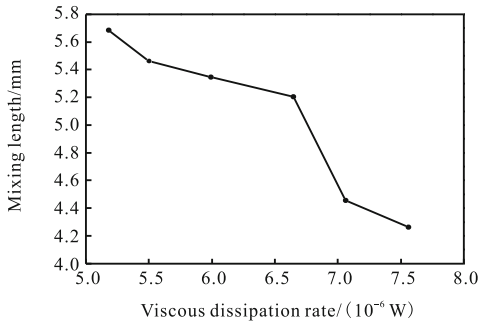

Fig. 7 Variation of the mixing length with the viscous dissipation rate

The mixing was expected to be augmented by the multi-vortices in the ideal velocity field. These secondary flows, in combination with the axial flow, distorted and stretched the interfaces and thereby improved the mixing. However, the mixing performance was improved accompanied by the increment of total viscous dissipation.

4 Realization of an ideal velocity field in mass transfer augmentation: The passive mixer

Since the mixing of optimized velocity field is greatly improved, it is advisable to achieve a mixing intensification via the realization of an ideal optimized velocity field. In this section, a procedure to produce the passive mixer with geometric irregularities is provided by employing the porous media model. As a necessary step, an optimized flow pattern has to be acquired. Note that the ideal velocity field is arbitrarily selected, and in this work, the optimized velocity field with ϕ of 6.649×10^{-6} W was selected.

For simple homogeneous porous media, the momentum sink S_i, which contributes to the pressure drop in the porous zone, is composed of two parts: a viscous loss term and an inertial loss term.

$$S_i = -(\frac{\mu}{\alpha}u_i + 0.5C_\gamma \rho |u_i| u_i) \tag{24}$$

For a laminar flow, the inertial loss term can be ignored compared with the viscous loss term. Therefore, the momentum sink in the porous media can be written as

$$S_i = -\frac{\mu}{\alpha}u_i \tag{25}$$

where α is the permeability of porous media.

In the solid zone, S_i tends to be negative infinity so that the velocity magnitude will be reduced to zero.

For the mathematic consideration, the sum of the squared error (SSE) defined in Eq. (26) justifiably reflects the degree of approximation between the real and ideal velocity fields.

$$\mathrm{SSE} = \sum_{i=x,y,z}(u_{i,\mathrm{real}} - u_{i,\mathrm{ideal}})^2 \tag{26}$$

where $u_{i,\mathrm{ideal}}$ and $u_{i,\mathrm{real}}$ are velocity components in ideal and real velocity fields, respectively.

For the solid zone, the SSE is:

$$\mathrm{SSE} = \sum_{i=x,y,z}(0 - u_{i,\mathrm{ideal}})^2 = \sum_{i=x,y,z}u_{i,\mathrm{ideal}}^2 \tag{27}$$

The difference in the SSE between the fluid cell and solid cell was applied to determining the need for replacing the fluid cell by a solid cell. Specifically, the region will be occupied by the solid cell if the SSE difference, $\sum_{i=x,y,z}(u_{i,\mathrm{real}} - u_{i,\mathrm{ideal}})^2 - \sum_{i=x,y,z}u_{i,\mathrm{ideal}}^2$, is larger than the threshold specified a priori; as such, the SSE between the real and ideal velocity fields can be reduced to a smaller or possibly minimum value in each step for a given number of solid cells. Therefore, the real velocity field was to some extent adjusted to the ideal field. Fig. 8 shows that the SSE increases with the increase of the fraction of solid phase because the ideal velocity field optimized by volume force cannot be realized exactly in the passive manner. The ideal velocity field is the result of the volume force field, which, given by Eq. (22), is in fact the necessary condition of the EDMA principle; while, in the designed mixer, the velocity field is passively adjusted by the resistance of the solid to the fluid.

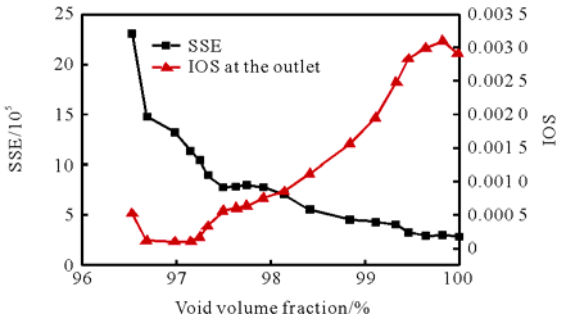

Fig. 8 Variation of SSE and IOS with the void volume fraction of fluid

The mixer still fails to achieve complete mixing. Consequently, the intensity of segregation (IOS)[32], as defined by Eq. (28), was used to quantitatively assess mixing efficiency.

$$\mathrm{IOS} = \sum_n \frac{(c - c_m)^2}{nc_m(1 - c_m)} \tag{28}$$

where n is the number of grid points at the outlet of the mixer.

As shown in Fig. 8, at first, the IOS increases with the increase of the number of solid cells, then it decreases and shows a minimum at the inflexion point corresponding to the void volume fraction of 97.15%. The designed mixer with a void volume fraction of 97.15% is displayed in Fig. 9. The comparison of the concentration field between the void tube and the mixer is shown in Fig. 10. The IOS of this mixer decreased to 1.077×10^{-4}, which is smaller compared with that of 2.783×10^{-3} in the void tube. However, the total viscous dissipation in the mixer was 3.832×10^{-5} W, which is larger than that of 3.282×10^{-6} W in the void tube. The comparison between the ideal optimized case and the real situation in the designed mixer is presented in Fig. 11 and Fig. 12, which also indicates that the significant difference in the augmentation mechanisms is mainly responsible for the obvious discrepancy.

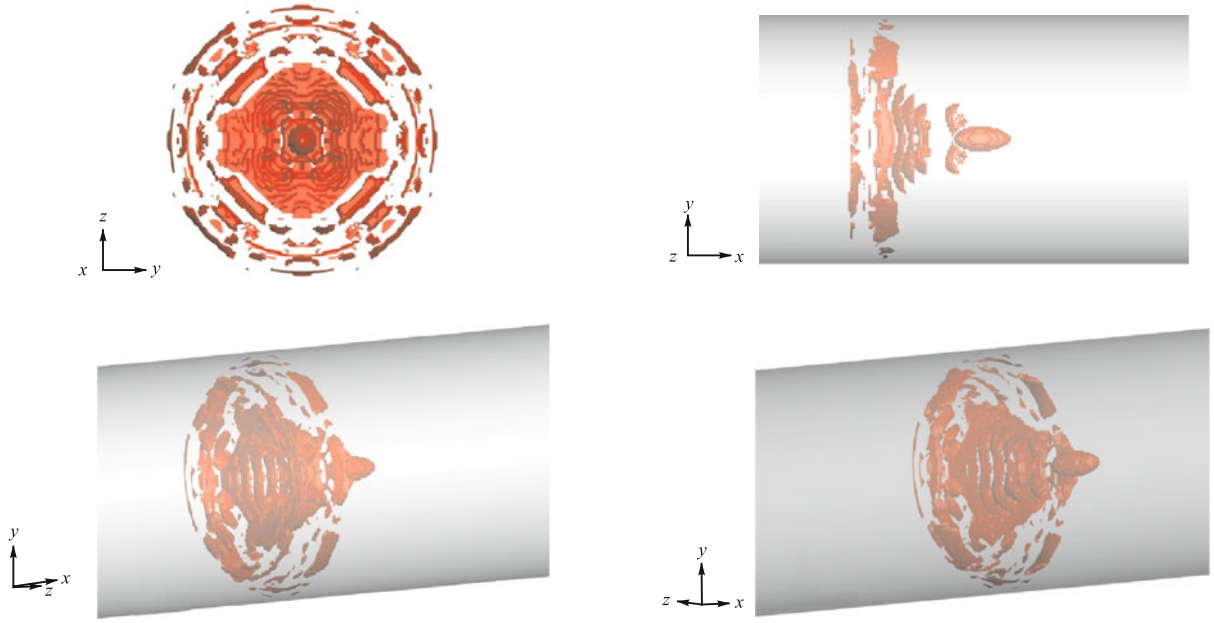

Fig.9 Sketch of the structure of passive mixer with geometric irregularities

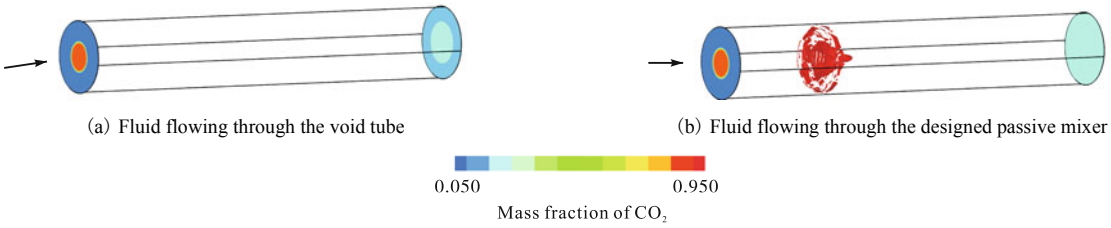

(a) Fluid flowing through the void tube (b) Fluid flowing through the designed passive mixer

Fig. 10 Contour of mass fraction of CO_2 at the outlet when fluid flowing through the void tube and the designed passive mixer

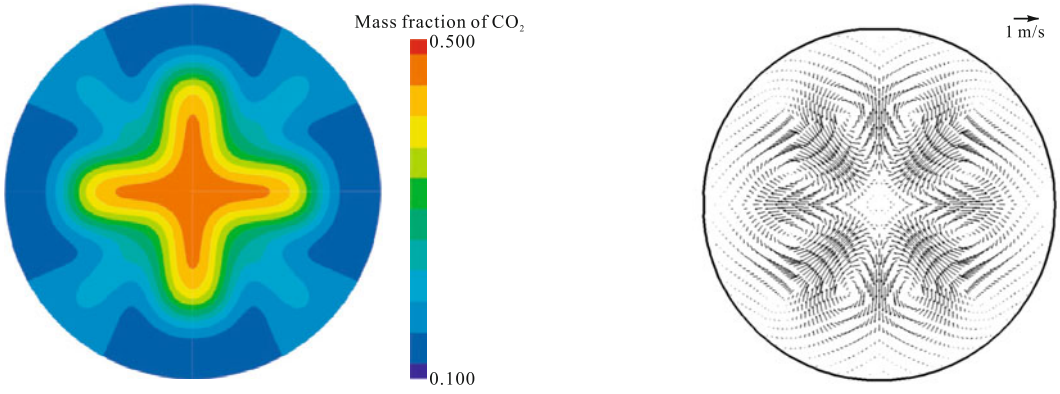

(a) Concentration field of CO_2 (b) Velocity field

Fig. 11 Concentration field of CO_2 and velocity field in the cross-section (x=2 mm) in the ideal optimized flow pattern

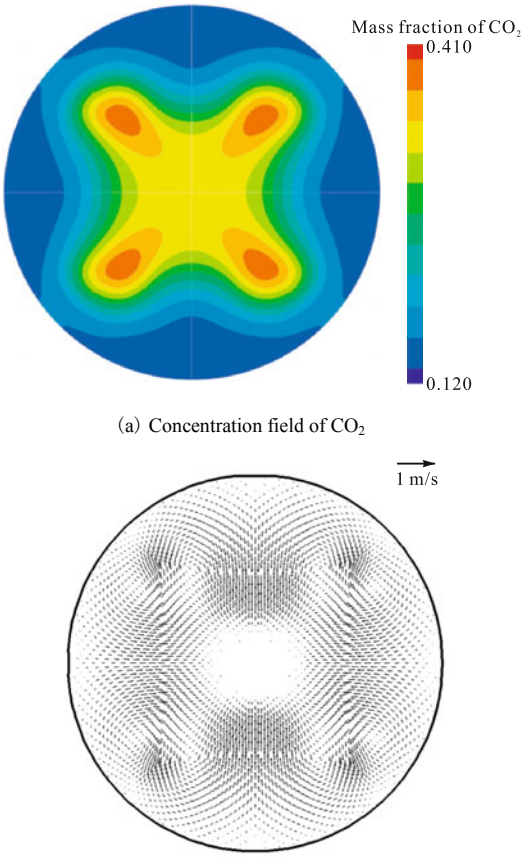

(a) Concentration field of CO_2

(b) Velocity field

Fig. 12 Concentration field of CO_2 and velocity field in the cross-section (x=2 mm) in the designed passive mixer

5 Conclusions

This study proposed the concept of DMA in convective mass transfer. Analogous to the heat-work conversion, the expression of DMA was derived. The optimization principle of EDMA was developed as a general approach to enhancing mass transfer.

The intensification of the mixing process for a gas mixture was provided to demonstrate the EDMA principle. We developed a mathematical model to formulate the mixing intensification into a variational problem, and performed the CFD modeling. The optimized flow pattern was obtained by solving the CFD model. In the course of simulation, the difference between the computation model here and an ordinary CFD model was the result of the volume force F, which modified the flow pattern and promoted the mixing. The complete mixing was achieved in the optimized ideal flow pattern due to the multi-vortices and secondary flows, but the viscous dissipation rate simultaneously increased.

The mixing performance of ideal optimized velocity field was satisfying so that it was reasonable and advisable to improve mixing by generating the optimized velocity field in a related apparatus. To this end, a specific procedure was provided to produce a passive mixer with geometric irregularities. The simulated results revealed that the IOS of the designed mixer decreased to 1.077×10^{-4}, which was smaller compared to that of 2.783×10^{-3} in the void tube. It should be clarified that the ideal optimized velocity field cannot be exactly realized by the available techniques at present. The ideal velocity field was the result of the volume force field; while in the produced mixer, the velocity field was passively adjusted by the resistance of the solid to the fluid. Apparently, due to the significant difference between the mechanisms of the mixing augmentation techniques, the real velocity field in the mixer still deviated from the optimized field. Nevertheless, the designed mixer provided the guideline for designing the efficient mixing element of the passive mixer in the conceptual stage.

References

[1] Bird R B. Five decades of transport phenomena [J]. *AIChE Journal*, 2004, 50(2): 273-287.

[2] Bird R B, Stewart W E, Lightfoot E N. *Transport Phenomena* [M]. John Wiley & Sons, New York, 2007.

[3] Leal L G. *Advanced Transport Phenomena*: *Fluid Mechanics and Convective Transport Processes* [M]. Cambridge University Press, Cambridge, 2007.

[4] Moulijn J A, Stankiewicz A, Grievink J *et al*. Process intensification and process systems engineering: A friendly symbiosis [J]. *Computers & Chemical Engineering*, 2008, 32 (1/2): 3-11.

[5] Gerven T V, Stankiewicz A. Structure, energy, synergy, time: The fundamentals of process intensification [J]. *Industrial & Engineering Chemistry Research*, 2009, 48(5): 2465-2474.

[6] Becht S, Franke R, Geißelmann A *et al*. An industrial view of process intensification [J]. *Chemical Engineering and Processing*: *Process Intensification*, 2009, 48(1): 329-332.

[7] Stankiewicz A. Reactive separations for process intensification: An industrial perspective [J]. *Chemical Engineering and Processing*: *Process Intensification*, 2003, 42(3): 137-144.

[8] Bejan A. A study of entropy generation in fundamental convective heat transfer [J]. *Journal of Heat Transfer*,

1979, 101(4): 718-725.

[9] Bejan A. *Entropy Generation Through Heat and Fluid Flow* [M]. John Wiley & Sons, New York, 1982.

[10] Bejan A. Second-law analysis in heat transfer and thermal design [J]. *Adv Heat Transfer* (United States), 1982, 15: 1-58.

[11] San J Y, Worek W M, Lavan Z. Entropy generation in convective heat transfer and isothermal convective mass transfer [J]. *Journal of Heat Transfer*, 1987, 109(3): 647-652.

[12] Ordóñez J C, Bejan A. Entropy generation minimization in parallel-plates counterflow heat exchangers [J]. *International Journal of Energy Research*, 2000, 24(10): 843-864.

[13] De Koeijer G, Rivero R. Entropy production and exergy loss in experimental distillation columns [J]. *Chemical Engineering Science*, 2003, 58(8): 1587-1597.

[14] Azoumah Y, Mazet N, Neveu P. Constructal network for heat and mass transfer in a solid-gas reactive porous medium [J]. *International Journal of Heat and Mass Transfer*, 2004, 47(14): 2961-2970.

[15] Ratts E B, Raut A G. Entropy generation minimization of fully developed internal flow with constant heat flux [J]. *Journal of Heat Transfer*, 2004, 126(4): 656-659.

[16] Johannessen E, Kjelstrup S. A highway in state space for reactors with minimum entropy production [J]. *Chemical Engineering Science*, 2005, 60(12): 3347-3361.

[17] Azoumah Y, Neveu P, Mazet N. Constructal design combined with entropy generation minimization for solid-gas reactors [J]. *International Journal of Thermal Sciences*, 2006, 45(7): 716-728.

[18] Ibáñez G, Cuevas S. Entropy generation minimization of a MHD (magnetohydrodynamic) flow in a microchannel [J]. *Energy*, 2010, 35(10): 4149-4155.

[19] Guo Z, Zhu H, Liang X. Entransy: A physical quantity describing heat transfer ability [J]. *International Journal of Heat and Mass Transfer*, 2007, 50(13): 2545-2556.

[20] Chen Q, Wang M, Pan N *et al*. Optimization principles for convective heat transfer [J]. *Energy*, 2009, 34(9): 1199-1206.

[21] Chen L, Wei S, Sun F. Constructal entransy dissipation rate minimization of a disc [J]. *International Journal of Heat and Mass Transfer*, 2011, 54(1): 210-216.

[22] Guo J, Xu M. The application of entransy dissipation theory in optimization design of heat exchanger [J]. *Applied Thermal Engineering*, 2012, 36: 227-235.

[23] Jia H, Liu W, Liu Z. Enhancing convective heat transfer based on minimum power consumption principle [J]. *Chemical Engineering Science*, 2012, 69(1): 225-230.

[24] Chen Q, Ren J, Guo Z. Field synergy analysis and optimization of decontamination ventilation designs [J]. *International Journal of Heat and Mass Transfer*, 2008, 51(3): 873-881.

[25] Chen Q, Meng J. Field synergy analysis and optimization of the convective mass transfer in photocatalytic oxidation reactors [J]. *International Journal of Heat and Mass Transfer*, 2008, 51(11): 2863-2870.

[26] Guo Z, Li D, Wang B. A novel concept for convective heat transfer enhancement [J]. *International Journal of Heat and Mass Transfer*, 1998, 41(14): 2221-2225.

[27] Liu Chunjiang, Zhao Ming'en, Guo Kai *et al*. Mixing equipment optimization based on flow pattern construction method [J/OL]. *Journal of Tianjin University*: Science and Technology. http:www.cnki.net/Rcms/detail/10.11784/tdxbz201401006.html. (in Chinese).

[28] Kavehpour H P, Faghri M, Asako Y. Effects of compressibility and rarefaction on gaseous flows in microchannels [J]. *Numerical Heat Transfer*, *Part A*: Applications 1997, 32(7): 677-696.

[29] Yu S, Ameel T A. Slip-flow heat transfer in rectangular microchannels [J]. *International Journal of Heat and Mass Transfer*, 2001, 44(22): 4225-4234.

[30] Massman W J. A review of the molecular diffusivities of H_2O, CO_2, CH_4, CO, O_3, SO_2, NH_3, N_2O, NO, and NO_2 in air, O_2 and N_2 near STP [J]. *Atmospheric Environment*, 1998, 32(6): 1111-1127.

[31] Gobby D, Angeli P, Gavriilidis A. Mixing characteristics of T-type microfluidic mixers [J]. *Journal of Micromechanics and Microengineering*, 2001, 11(2): 126-132.

[32] Danckwerts P V. The definition and measurement of some characteristics of mixtures [J]. *Applied Scientific Research* (*Section A*), 1952, 3(4): 279-296.

(Editor: Zhao Yang)